7 EXCLUSIVE η RECONSTRUCTION

In this chapter the procedure to identify the η meson decays will be presented. The study of the η meson is of particular interest for several reasons. The inclusive η cross section is well known in the vicinity of the production threshold, but at higher energy the experimental values have large errors and they can be significantly improved (see paragraph 2.5).

The η production cross section can be measured both through the hadronic ($\eta\rightarrow\pi^+\pi^-\pi^0$) and the dielectron ($\eta\rightarrow e^+e^-\gamma$) Dalitz decays, whose branching ratios are known. This fact allows to use the $pp\rightarrow pp\eta$ channel as a calibration reaction for the dielectron identification of the spectrometer, in order to normalize the dielectron yields in the heavy ions experiments. Moreover an accurate measurement of the η Dalitz decay could help improving our evaluation of the electromagnetic form factor of the meson.

7.1 Particle identification

In order to perform an exclusive reconstruction we need to identify all the charged particles in the exit channel.

We are interested in reconstructing the η hadronic decay into three pions $pp\eta\rightarrow pp\pi^+\pi^-\pi°$, and the electromagnetic Dalitz decay $pp\eta\rightarrow pp e^+e^-\gamma$; thus we need to identify in an event two protons and two pions for the hadronic decay, two protons and a lepton pair in the electromagnetic case.

The lepton identification can be performed by using the correlation of the track with the RICH detector: if the particle provides a signal in the RICH which can be identified as a ring, we can assume that the selected particle is an electron or a positron according to its charge (from the trajectory deflection inside the magnetic field region).

The hadron identification is usually done by a correlated measurement of momentum and velocity of the particles, but in order to use this kind of algorithm we need a correct time of flight measurement. After the start time reconstruction method, explained in chapter 6, we have reliable values of particle velocity which can be used for this purpose.

In the analysis of this chapter only the Runge Kutta tracking algorithm will be used for angle and momentum reconstruction, because of its improved performances respect to Spline algorithm.

For the η hadronic decay we need to identify two protons and two pions. The left side of Figure 7.1 shows the momentum times polarity versus β distribution in experimental data, for events where the start time was reconstructed from a negative pion. We do not need to analyse events which contain leptons, so we can take them out of our sample.

The hadron identification is performed by a graphical cut on the two dimensional distribution. The selection is quite broad in order not to lose efficiency at this stage of the analysis; by imposing constraints from the kinematics of the desired reactions we will be able to remove wrongly identified tracks.

For the η electromagnetic decay we need to identify two protons and a lepton pair. The right side of Figure 7.1 shows the same momentum versus β plot, but this time for events where the start time was reconstructed from an identified lepton.

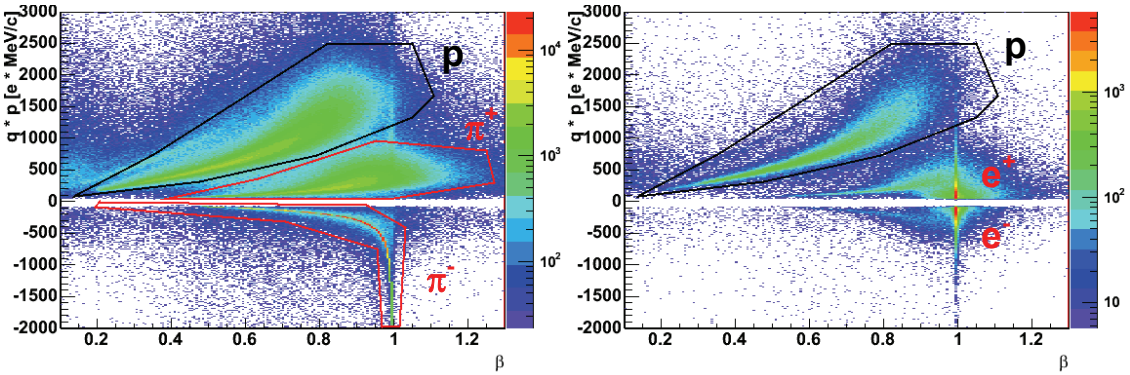

Figure 7.1 – Momentum times polarity versus β distributions for the January 2004 experimental data, in cases where the start time is reconstructed by an identified π^- (left plot) and by an identified lepton (right plot). The graphical selections for hadron identification are indicated.

In this case we only need to identify the proton region by the same graphical selection used for the hadronic decay.

In order not to lose statistics the lepton identification was performed by using only RICH correlation, without imposing conditions on the ring quality (minimum bias) and without detecting electromagnetic showers in the Shower detector. Even in this case the misidentified tracks will be removed by further conditions on the kinematics of the event.

For exclusive η reconstruction in experimental data only events with the M4smart[1] 1st level trigger selection were analysed (about 265 millions).

The event reduction after applying several conditions is shown in Figure 7.2, in comparison for experimental and simulation data samples. The numbers can also be read in Table 7-1.

The first condition consists on a selection of events which contain at least three positive and one negative charged particles [(+)>2 && (-)>0]; we can see that this condition strongly reduces the statistics for both the simulation and experimental data samples.

From these numbers we can see that the surviving events after this selection are about 3.2% of the total events for experimental data, while about 1.9 % in simulation. This reflects the fact that in experiment we are much more dominated by secondary particles which are not present in simulation; these tracks are fully reconstructed by the tracking system and increase the number of events inside the selections.

Selection	Explanation	simulation	experiment
M4smart	Trigger selection	155,132,559	263,067,265
(+)>2 && (-)>0	3 positive 1 negative particles	3,005,423	8,335,245
tofrec !=0	Start time reconstruction	2,866,133	7,785,520
p > 1	Two identified protons	2,009,247	5,386,906
pi+ pi-	Two protons and two pions	1,709,904	3,858,643
e+ e-	Two proton and a lepton pair	38,624	115,311

Table 7-1 – Table of event reduction after different kind of selections.

[1] M4smart condition means: at least four particles in META detector, at least two particles in TOFINO detector, and two META opposite sectors hit.

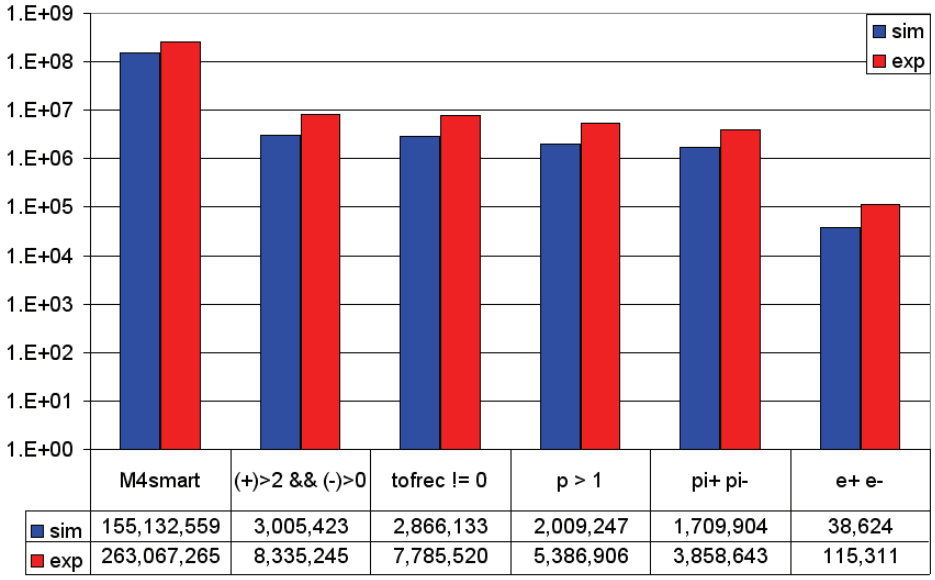

	M4smart	(+)>2 && (-)>0	tofrec != 0	p > 1	pi+ pi-	e+ e-
sim	155,132,559	3,005,423	2,866,133	2,009,247	1,709,904	38,624
exp	263,067,265	8,335,245	7,785,520	5,386,906	3,858,643	115,311

Figure 7.2 – Event reduction after applying several conditions in order to perform exclusive η meson reconstruction, for both simulation and experimental data samples (see the text and Table 7-1).

On a second step we need to impose that the start time is reconstructed [tofrec != 0], in order to perform particle identification by using momentum and velocities. We can see that the event reduction by requiring time reconstruction is minimal, thus meaning that the global efficiency of the start time reconstruction algorithm is quite high.

By using the reconstructed start time we can apply the graphical selection to identify particles. First we select events with at least two protons[2] [p > 1]; then we can search events which contain at least one π^+ and one π^- [pi+ pi-] for hadronic decay, or one electron and one positron [e+ e-] for electromagnetic decay. In the latter case we can see a strong reduction in number of events, considered the low branching ratio for dilepton production.

After we have identified all the four charged particles the event is not yet fully reconstructed, because we are still missing one particle: a neutral pion in the hadronic decay, and a photon in the electromagnetic decay. The missing particle can be found by means of a missing mass analysis.

In order to calculate the missing mass of the system we need to know energy and momentum values of the particles in the initial state and in the exit channel.

The initial state of the reaction is defined by the 4-momentum of the projectile plus the 4-momentum of the target ($E_{ini} = E_{proj} + m_{target}$, $\vec{p}_{ini} = \vec{p}_{proj}$), thus it is substantially fixed by the beam energy. Momenta for the outgoing particles $\vec{p}_{out}$ are provided by the tracking system, while the energy is calculated by $E_{out} = \sqrt{p_{out}^2 + m^2}$, where the mass *m* is the value assumed from the particle identification.

Thus we can express the missing mass (squared) by the formula:

$$M^2 = \left(E_{ini} - \sum_i E_{out}^i \right)^2 - \left(\vec{p}_{ini} - \sum_i \vec{p}_{out}^i \right)^2 \qquad \textbf{(Eq. 7-1)}$$

[2] Physically we cannot have more than two protons in the event, but experimentally we have proton multiplicities even larger than two due to particle misidentification.

where the sum is extended over the detected particles in the exit channel, the two outgoing protons in the case of the missing η or the four particles $pp\pi^+\pi^-$ - ppe^+e^- respectively for the missing pion or photon.

In the following paragraphs the exclusive reconstruction procedure will be shown separately for hadronic and electromagnetic decays.

7.2 η hadronic decay

In this chapter the procedure to identify η mesons decaying into hadrons will be explained.

Using the momentum versus velocity plot of Figure 7.1 (left side) it is possible to identify the particles and to select 4-prong events where two protons, a negative pion and a positive pion are detected; by looking at the missing mass distribution it is then possible to select events with the hadronic decay of the η meson.

The reaction of interest is $pp \rightarrow pp\eta \rightarrow pp\pi^+\pi^-\pi^0$. If we plot the missing mass distribution of the four-particle final state we should observe a peak in the region of the missing neutral pion; moreover, by plotting the missing mass of the two protons of the final state, the peak of the missing η meson should appear.

The analysis will be shown separately for simulation and for experimental data.

7.2.1 Simulation

Figure 7.3 shows the *pp* squared missing mass (y axis) versus $pp\pi^+\pi^-$ squared missing mass (x axis), for the simulation data sample.

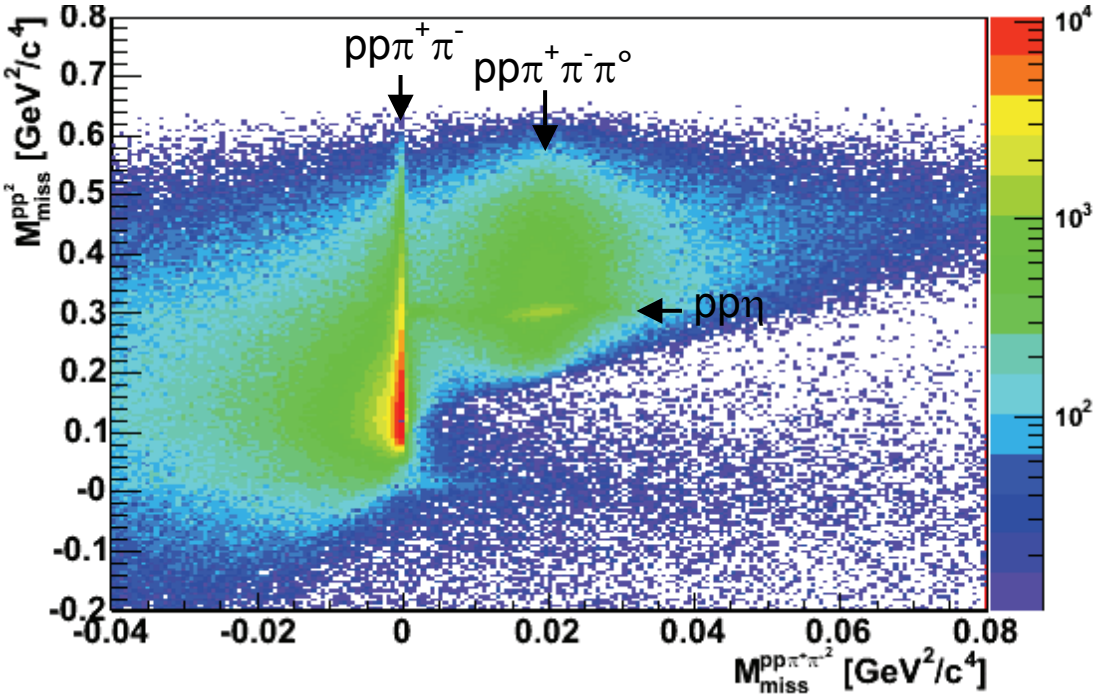

Figure 7.3 – Missing mass plot for four detected particles (two protons, two pions), in simulation. All the visible reaction channels are indicated in the plot.

The simulation is not so close to the experiment, due to an imperfect handling of the detector alignment in the experimental data and to some effects not yet considered in simulation (see chapter 5 for the details), but it provides important hints on what we should expect and what we find in real data.

Looking at the plot one observes that the main part of the distribution stays around the zero value of the four-particles missing mass; this corresponds to the $pp \to pp\pi^+\pi^-$ channel fully reconstructed (no missing particles).

In the positive region of the x axis there is a prominent bump, corresponding to events where the π^0 is missing. In this region the η meson appears as a peak in the two-proton missing mass, in form of a horizontal trace in the plot.

In order to identify η mesons the first step is to find events with a missing π^0. If we look at the $pp\pi^+\pi^-$ missing mass distribution of Figure 7.4, in a mass range between 30 MeV/c^2 and 350 MeV/c^2 in order to cut out the strong contribution coming from the $pp \to pp\pi^+\pi^-$ channel (peaked at zero), we can see that the missing π° peak is quite evident.

The background contamination is quite low. In order to find the peak position and an estimate of the 4 particles mass resolution we can fit the distribution with a gaussian function (in red) for the main peak, plus a polynomial function (in green) to fit the background; the resulting function is shown in black.

We can see that the correspondence between the fit function and the measured distribution it is not optimal, but it allows to obtain a rough estimate.

The fit result shows that the peak position is centred at 139 MeV/c^2 with a width of 19 MeV/c^2, close to the effective π° mass of 135 MeV/c^2 (within the error bars). From the width we can estimate the resolution for the invariant mass measurement made using four particles ($pp\pi^+\pi^-$); the obtained value is 13.7%.

By imposing a cut around the peak region we can select events with the missing π°, and then we can look at the distribution of the two-proton missing mass.

The selected range of four-particle missing mass is between 50 MeV/c^2 and 250 MeV/c^2. The cut is quite broad in order not to lose missing π° events; the efficiency of the cut is estimated close to 100% for our analysed reaction, so we do not have a strong reduction of η signals from this selection.

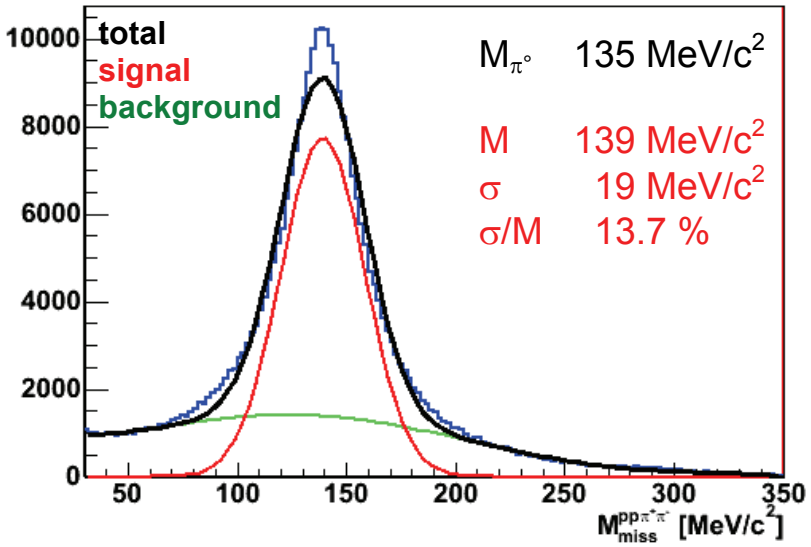

Figure 7.4 – Simulation plot of $pp\pi^+\pi^-$ missing mass distribution between 30 MeV/c^2 and 350 MeV/c^2, in order to discard the contribution from the $pp \to pp\pi^+\pi^-$ channel. The missing π° peak is prominent.

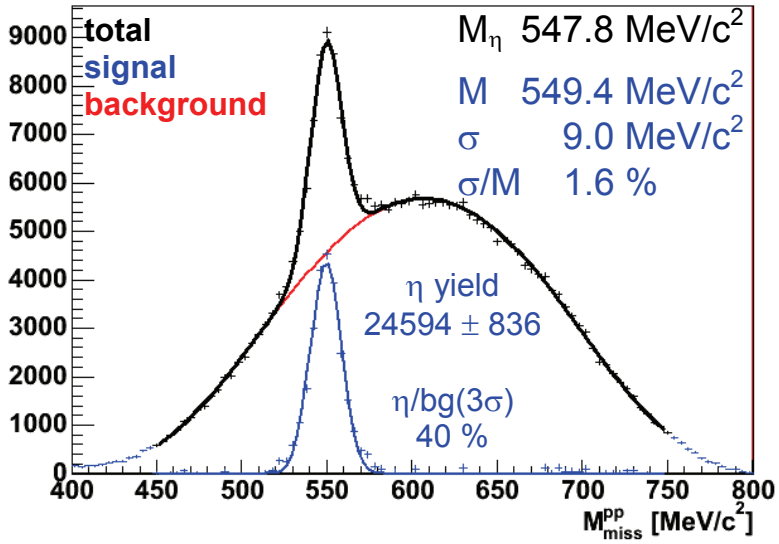

Figure 7.5 – Proton-proton missing mass distribution for simulation data, after the selection on 4 particle missing mass in the range [50 MeV/c^2, 250 MeV/c^2]. Results from a fit with a gaussian (η signal) plus a polynomial (background) functions are reported, as well as total yield and signal/background (bg) ratio in a 3σ mass window around the η peak.

Figure 7.5 shows the proton-proton missing mass distribution, after the missing π° selection (black dots). The error bars in the plot come from statistical error.

The spectrum is composed of the physical background, coming from $pp\pi^+\pi^-\pi^0$ non-resonating channel, plus the well defined peak of the missing η meson.

The distribution can be fitted in order to estimate the peak position, the mass width and the η meson yield. The function (black line) used for the fit was a gaussian for the signal (blue line) plus a polynomial to fit the background (red line).

In this case we see a good agreement between the fit function and the measured distribution. The blue dots represent the estimated η signal, thus the measured distribution less the background fit function.

The peak is located at 549.4 MeV/c^2, i.e. at the theoretical position (m_η=547.8 MeV/c^2); the width of the gaussian function is 9.0 MeV/c^2, which corresponds to a two-particle invariant mass resolution of 1.6%.

By integrating the signal fit function over a mass range between 500 MeV/c^2 and 600 MeV/c^2, reasonably broad with respect to the estimated peak in order not to lose η signal events, we obtain a yield of 24594 ± 836 η mesons[3] for the full simulation sample.

It is possible to estimate the signal over background ratio in the η meson mass range. The calculation was done over a 3σ mass window around the η peak; an η yield of 24527 was obtained (close to the value obtained by integrating over the [500,600] MeV/c^2 mass range), while 60756 counts were estimated as the background yield. By dividing these two numbers we obtain about 40% as signal to background ratio.

We can therefore state that in simulation it is possible to identify the η meson by using this missing mass technique.

[3] The errors are computed by propagating parameter errors coming from the signal's gaussian fit inside the integral function.

But now we want to apply the same procedure in experimental data, which are affected by a worse momentum resolution, and thus we should expect a worsening in terms of resolution and signal to background ratio.

7.2.2 Experimental data

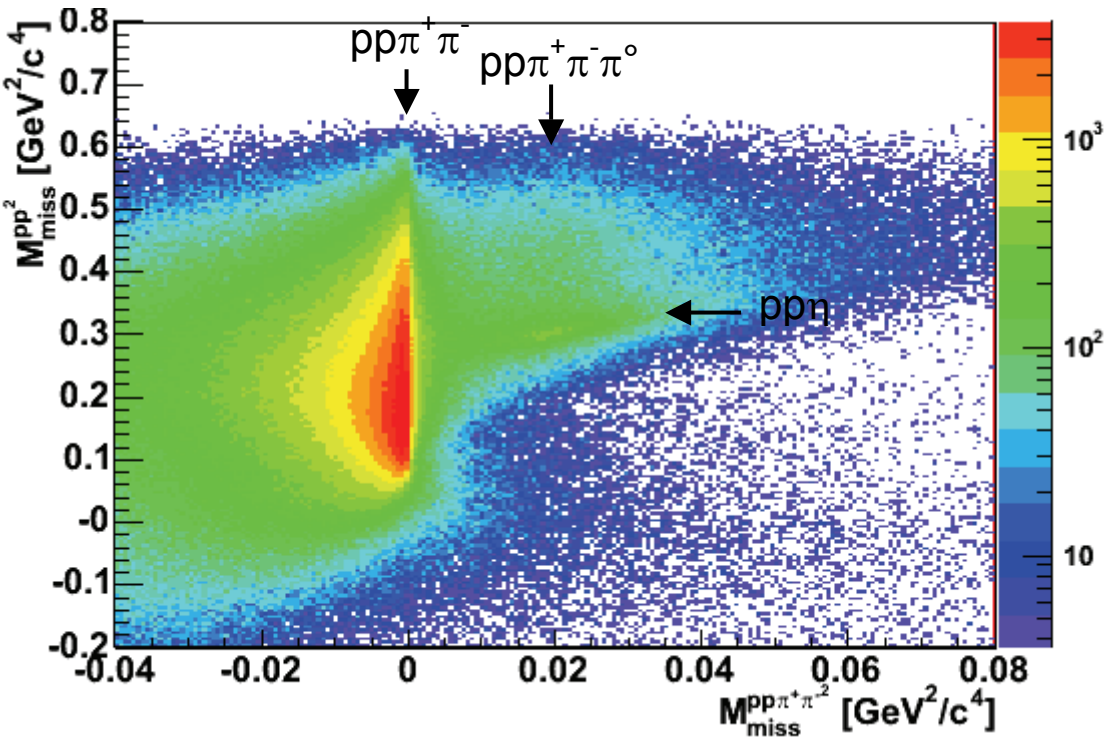

Figure 7.6 – Missing mass plot for four detected particles ($pp\pi^+\pi^-$), in experimental data. All the visible reaction channels are indicated.

Figure 7.6 shows the two-dimensional missing mass plot for the January 2004 experimental data sample.

We can see the worse momentum resolution compared to the simulation data (see chapter 5 for differences between momentum resolution in simulation and in experiment); the distributions are broader and the separation between the $pp\pi^+\pi^-$ channel and the $pp\pi^+\pi^-\pi^\circ$ channel is not so well defined as in the simulation case (see Figure 7.3). Nevertheless the $pp\eta$ channel is still evident in the plot as well as the missing π°, so the exclusive η reconstruction procedure can be performed also in the experimental data.

First of all only downscaled events (LVL1) were used for the data sample; not downscaled events (LVL2) contain at least a lepton pair and we are not interested in analysing them. In this way, if we calculate the η yield in downscaled events, by multiplying this number times the average downscaling factor we get an estimate of the total number of η meson events (via hadronic decay) which passed the 1st level trigger selection (see paragraph 4.6.1).

After selecting downscaled events, we can plot the $pp\pi^+\pi^-$ missing mass distribution as shown in Figure 7.7. In order to reduce possible sources of background events, an additional condition was put in the proton-proton missing mass, by selecting a range between 400 MeV/c^2 and 800 MeV/c^2.

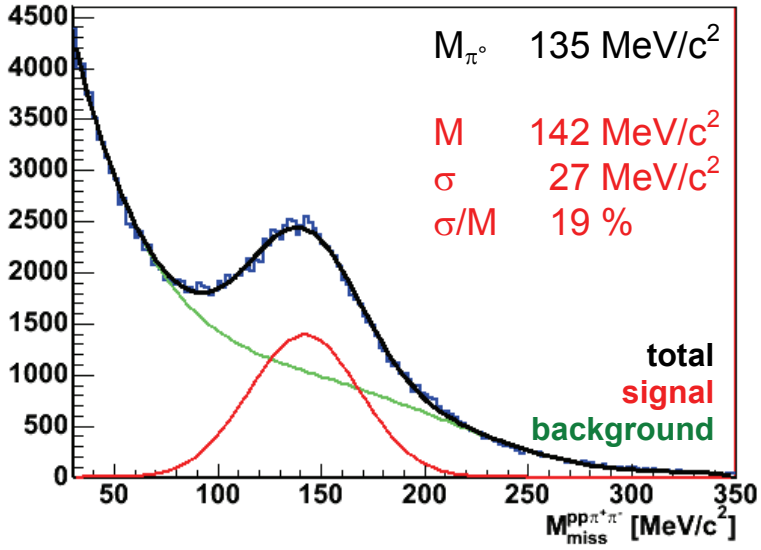

Figure 7.7 – $pp\pi^+\pi^-$ experimental missing mass distribution, after a selection on pp missing mass between 400 MeV/c^2 and 800 MeV/c^2. The background from the $pp\pi^+\pi^-$ channel is higher than in the simulation case, but the missing π° peak is still visible. The distribution was fitted (black line) with the sum of a gaussian function (red line) for the π°, and a polynomial (green line) for the background.

In experimental data we can see that the contribution from $pp\pi^+\pi^-$ channel is much higher, mainly due to the worse momentum resolution; however the missing π° peak is visible and can be selected.

The experimental distribution was fitted (black line) as in the simulation data, with the sum of a gaussian (red line) for the π° signal plus a polynomial function (green line) for the background.

By looking at the fit results, the π° mass peak is centred at 142 MeV/c^2 with a width of 27 MeV/c^2, which corresponds to 19% as invariant mass resolution.

The peak is close to the π° mass value within error bars; the resolution is broader than in simulation, as we expect from the different momentum resolution.

In order to select events with a missing π°, the same 4 particle missing mass selection applied in simulation was used, thus a mass range between 50 MeV/c^2 and 250 MeV/c^2, which corresponds to about a 3.7 σ selection around the π° peak. If we assume that the π° follows a gaussian distribution, we should not lose π° signal events by applying this mass selection (below 0.1%).

The obtained pp missing mass distribution is reported in Figure 7.8. The shape is similar to what obtained in simulation, the η peak is visible but broader, while the background in the low mass region of the distribution is higher, mainly due to the higher contamination from $pp\pi^+\pi^-$ decay channel. The error bars are given by statistical errors.

The distribution was fitted (black line) with a gaussian function for the η peak (blue line) plus a polynomial function for the background (red line). The black dots represent the experimental distribution, while the blue dots correspond to the distribution less the background fit function. We can see that the obtained function fits well the experimental distribution, even if there is a small discrepancy in the higher mass tail of the η signal peak.

The η peak is centred at 554.1 MeV/c^2 with a width of 19.7 MeV/c^2; the obtained missing mass resolution is 3.5%, which is enough to distinguish the η peak.

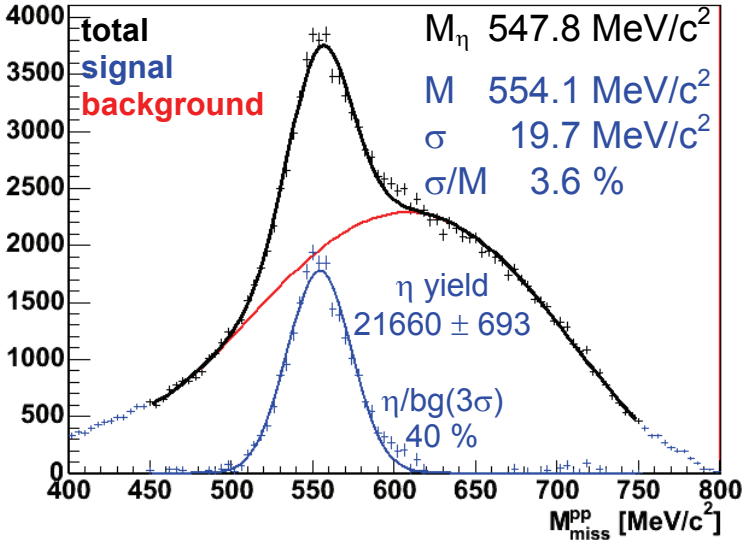

Figure 7.8 – Proton-proton missing mass distribution for experimental data, after the selection on four particle missing mass [50 MeV/c^2, 250 MeV/c^2]. The fit function (black line) is the sum of a gaussian (η signal) plus a polynomial (background) function. Fit results, η yield and signal/background (bg) ratio are reported.

By integrating the signal fit function between 500 MeV/c^2 and 600 MeV/c^2 (about 3.6 σ selection, so by assuming an η meson gaussian distribution the signal reduction should be lower than 0.1%), we obtain 21670 ± 693 η signals.

The signal over background ratio was estimated by calculating the signal and the background yield in a 3σ missing mass region around the η signal peak. We obtain 21883 η signal events (almost the same of the [500,600] MeV/c^2 selection) and 55270 background events; by dividing these two numbers we can estimate a signal/background ratio of about 40%, similar to what obtained in simulation.

To conclude the hadron decay channel analysis we can calculate the total number of η hadronic decays which passed the 1st level trigger selection. All the obtained numbers were calculated only for the downscaled data sample; by multiplying the total yield by the average downscaling factor 2.2 (see paragraph 4.6.2), we obtain a total of 47674 ± 1525 η hadronic decays, without any acceptance corrections.

We can rightfully state that the exclusive reconstruction of the η hadronic decay is possible by means of the HADES spectrometer.

The obtained values of resolution and signal/background ratio can be improved by applying a refinement method, the kinematic refit.

7.2.3 Kinematic refit

The kinematic refit is a procedure to improve the tracking parameters of the particles which concur in a physical reaction, by imposing kinematic constraints.

Let us assume to have a set of parameters provided by the tracking system, which for a particle can be expressed by momentum p, polar and azimuthal angles θ and ϕ. We can express this set of tracking parameters as[4]:

[4] We use as track parameter $1/p$ instead of p because it follows a gaussian distribution, a mandatory condition for the kinematic refit procedure

$$\alpha_i = (1/p, \theta, \phi)^T \qquad \textbf{(Eq. 7-2)}$$

In our case α_i are the tracking parameters of the four particles needed for the exclusive η reconstruction.

In order to reconstruct the η meson a condition can be imposed on the missing mass of the four particles, which should corresponds to the mass of a π° meson.

A kinematic refit procedure varies the α tracking parameters of all the particles (3 parameters for each of the four particles, so in total 12 parameters) until the best values $\tilde{\alpha}$ are found which satisfy the imposed constraint.

The constraint is imposed by using the Lagrange multiplier method. In mathematical form, this procedure requires the minimization of the functional F:

$$F = \left(\vec{\alpha} - \vec{\tilde{\alpha}}\right) W^{-1} \left(\vec{\alpha} - \vec{\tilde{\alpha}}\right)^T + \lambda^T H(\tilde{\alpha}) \qquad \textbf{(Eq. 7-3)}$$

where W is the error matrix, λ is the Lagrange multiplier and H is the physical constraint on the four particles missing mass[5].

In order to perform the kinematic refit we need to know the error values of the W matrix. The errors on angular variables such as θ and ϕ are given by the propagation of errors from the time fits in the drift chambers; these values were multiplied by two in order to take into account a worse angular resolution coming from the small misalignment. The errors on the momentum reconstruction were set sectorwise by using the values obtained in the elastic scattering analysis of chapter 5, separately for simulation and for experimental data.

The analysis procedure for the kinematic refit remains the same as explained before; the four particle missing mass selection between 50 MeV/c^2 and 250 MeV/c^2 is done on the original mass value; the refitted one cannot be used because it is affected by the imposed kinematic constraint.

In Figure 7.9 the comparison between the pp missing mass distribution before and after applying the kinematic refit is shown, for simulation and for experimental data.

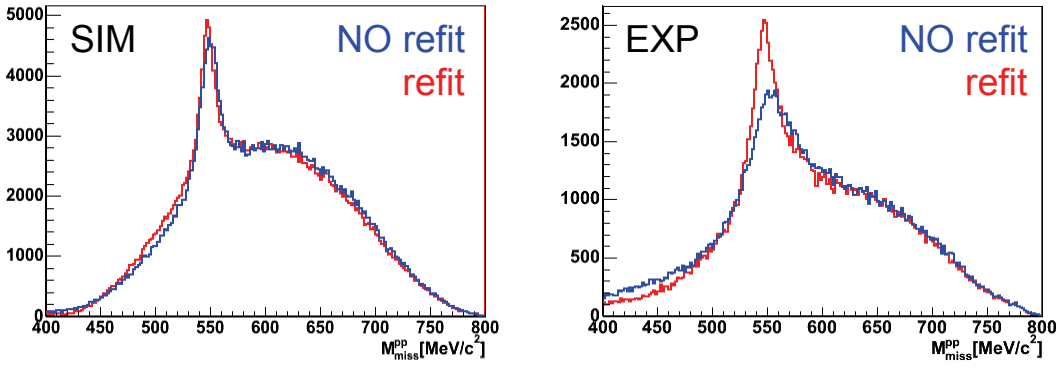

Figure 7.9 – Proton-proton missing mass distributions for simulation (left) and experimental data (right). It is possible to see the comparison between the distribution with and without kinematic refit.

[5] If we want to impose not one but n physical constraints, λ and H become $\lambda = (\lambda_1, \lambda_2, ..., \lambda_n)^T$, $H = (H_1, H_2, ..., H_n)$.

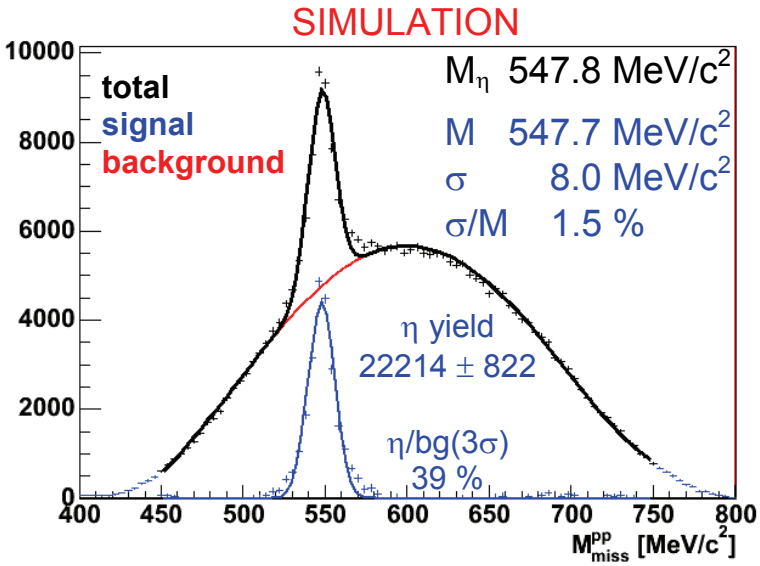

Figure 7.10 – Pp missing mass distribution for simulation, after the kinematic refit.

In simulation it seems that there is no strong improvement in the distribution. The background changes a bit its shape and the η peaks becomes a little narrower. But if we look at the experimental distribution, the kinematic refit improves a lot the missing mass distribution, the η peak is narrower and we have more counts around the peak region.

Now the usual fit procedure can be applied to the pp missing mass distributions, in order to estimate the new values of the peak position, of the mass width and of the signal to background ratio.

Figure 7.10 shows the distribution for simulation data. The peak is centred at 547.7 MeV/c^2, it is closer to the correct value and the width decreases by 1 MeV/c^2, moving at 8 MeV/c^2 which corresponds to a mass resolution of 1.5%.

Under the signal peak in the [500,600] MeV/c^2 mass range we obtain an η yield of 22214 ± 822, while the new signal to background ratio in a 3σ mass window is 39%.

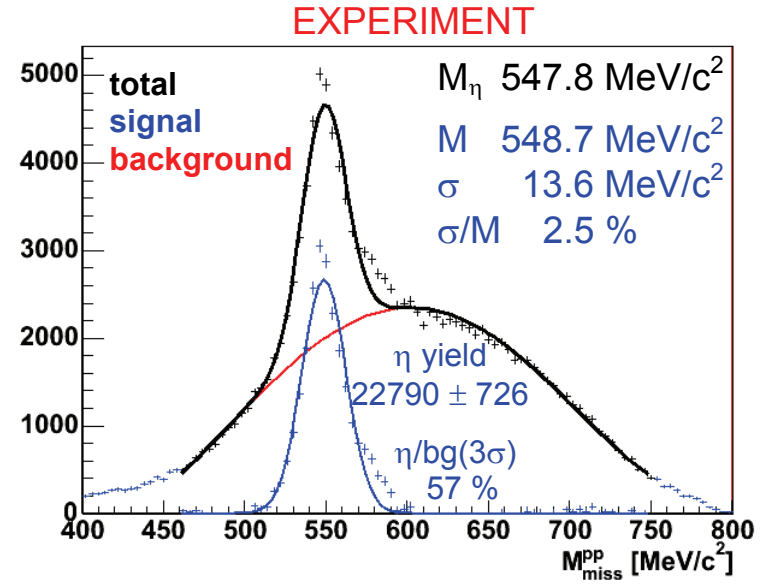

Figure 7.11 – pp missing mass distribution for experimental data, after kinematic refit.

We can state that the improvement is minimal and only in terms of mass resolution. The number of counted η mesons is a bit lower than the old value (even if within the error bars), and the signal/background ratio dropped by one percent. The reason of these reductions can be found by looking at the background subtracted mass distribution (blue dots) and the signal fit function in the plots. After applying the kinematic refit the signal peak is not well fitted by the gaussian in the tail regions, and even at the peak centroid; we can easily see that the fit is underestimating the correct number of η mesons, and then the obtained numbers reflect this feature.

Figure 7.11 shows the experimental distribution after the kinematic refit. Here the improvement is well visible. After the refit the η peak is at 548.7 MeV/c^2, much closer to the theoretical value, while the mass width decreases from 19.7 MeV/c^2 (3.6%) to 13.6 MeV/c^2 (2.5%).

This improvement in the mass resolution affects also the η yield. In the mass region between 500 MeV/c^2 and 600 MeV/c^2 we count 22790 ± 726 η signal events, and the signal/background ratio is now 57% in a 3σ mass region around the η peak. This means that, in the experimental data, by means of a kinematic refit the η signal becomes higher than the background events, as we can easily see from the distribution. Moreover the little higher number of η mesons reconstructed after the kinematic refit shows that the procedure is able to recover events which were rejected by simply using Runge Kutta tracking algorithm, moving them in the correct position under the peak.

In order to evaluate the number of η signal events which passes the 1st level trigger selection, we must multiply the yield by the average downscaling factor 2.2.

In this case we obtain as total number of η events a yield of 50138 ± 1597, which will have to be compared to the numbers obtained from the electromagnetic decay.

Coming back to the signal fit, here we can see problems in the gaussian fit of the signal distribution (blue dots), which become more pronounced toward the higher mass tail and at the peak position. In spite of the good results obtained in the hadronic exclusive reconstruction, this problem remains open for a more refined analysis.

Table 7-2 shows a summary of all the results obtained for the exclusive reconstruction of η meson hadronic decay, for simulation and experimental data, before and after applying a kinematic refit.

		Mass [MeV/c^2]	σ [MeV/c^2]	σ/M [%]	η yield	η/bg [%]
SIM	NO refit	549.4	9.0	1.6	24594±836	40
	refit	547.7	8.0	1.5	22214±822	39
EXP	NO refit	554.1	19.7	3.6	21660±694	40
	refit	548.7	13.6	2.5	22790±726	57

Table 7-2 – Summary of the results for the exclusive reconstruction of the η hadronic decay.

7.3 η electromagnetic decay

In this chapter the procedure to perform the exclusive reconstruction of the electromagnetic decay of η mesons will be explained.

The particle identification via the momentum versus velocity plot of Figure 7.1 (right side) is used only for protons; electron and positron are identified by requiring the correlation of their tracks with a recognized pair of rings in the RICH detector.

After the particle identification, the same procedure applied for the hadronic decay will be followed for the electromagnetic case, that is looking at missing mass distributions and searching for missing particles.

The reaction of interest is $pp \rightarrow pp\eta \rightarrow pp e^+ e^- \gamma$. If we plot the missing mass distribution of the 4-particle final state we should observe a peak centred at zero, corresponding to the missing photon; moreover, by plotting the missing mass of the two proton final state, we should search the missing η meson peak.

The analysis will be shown separately for simulation and for experimental data, and the kinematic refit will also be used to improve the results.

7.3.1 Simulation

In Figure 7.12 we can see the pp squared missing mass (y axis) versus $pp e^+ e^-$ squared missing mass (x axis) distribution, for the simulation data sample.

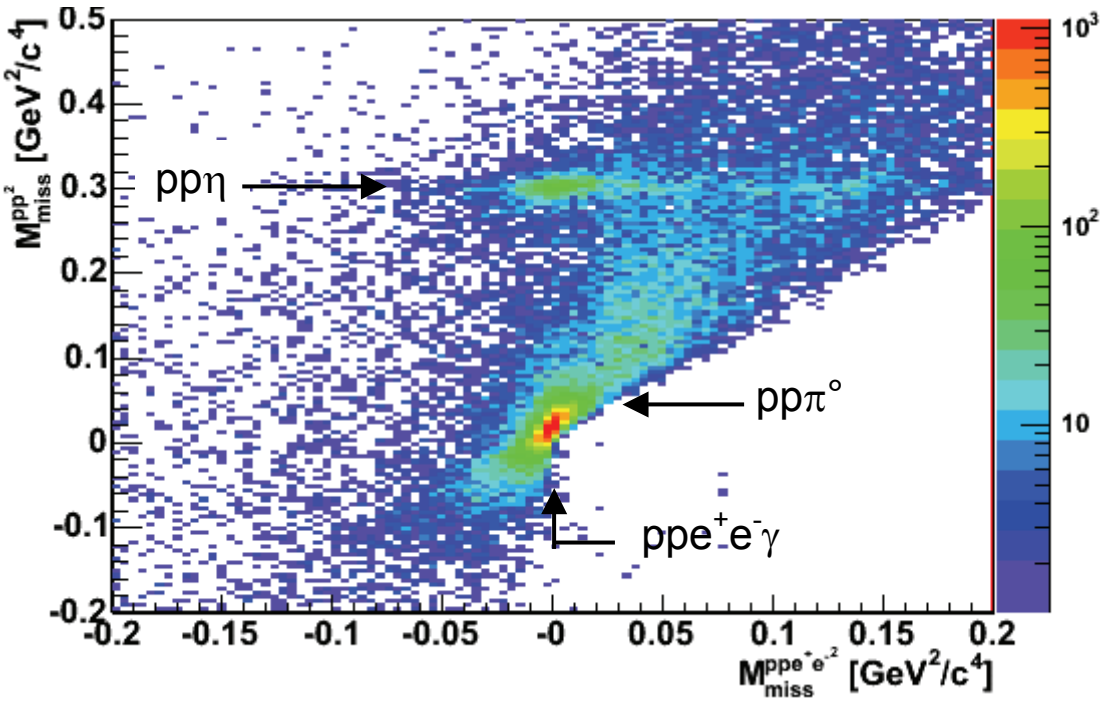

Figure 7.12 – Missing mass plot for four detected particles (two protons, two leptons), in simulation. All the visible reaction channels are indicated in the plot.

In the plot most of the counts are placed at $pp e^+ e^-$ missing mass values close to zero, which are related to the missing photon; from the statistics we have in the data sample the number of direct decay processes $pp \rightarrow pp e^+ e^-$ is almost negligible. The low pp missing mass region is mainly dominated by ppπ° reactions, while the η meson region is well separated and visible at higher mass values.

First of all we must select events where a photon is missing. This can be done by plotting $pp e^+ e^-$ missing mass distribution.

In order to reduce the contribution from background reactions, a selection on proton-proton squared invariant mass close to the η bump was used, between 0.27

GeV^2/c^4 and 0.33 GeV^2/c^4; in this way the position of the missing γ peak and its width can be evaluated.

In Figure 7.13 the ppe^+e^- missing mass (squared) distribution is shown, after this selection; the missing γ peak is well visible over the background. The distribution was fitted by a polynomial function for the background (red line) plus a gaussian for the main peak (blue line); the fit results are shown in the plot.

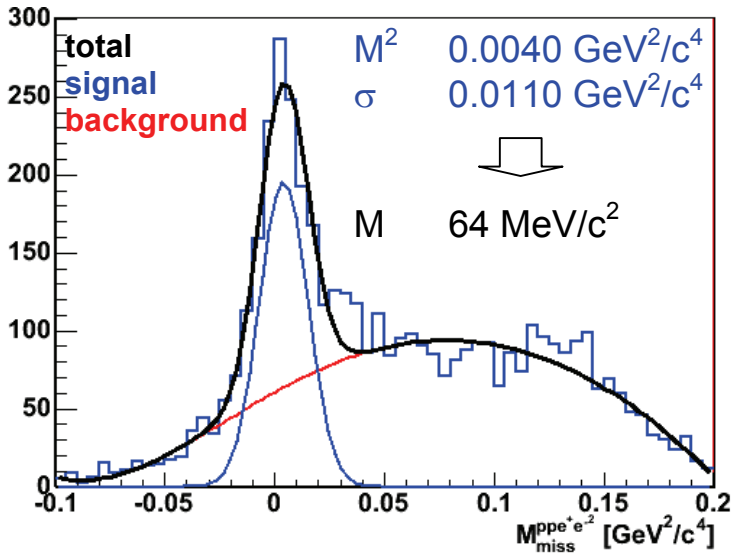

Figure 7.13 – ppe^+e^- missing mass squared distribution close to the η bump, for simulation data ($0.27\,GeV^2/c^4 < M^{2}_{miss}{}^{pp} < 0.33\,GeV^2/c^4$).

From the square root of the peak position we can evaluate the corresponding value of missing mass. We can see that the peak is not centred at zero but at a little higher mass value, about 65 MeV/c^2.

We can compare the obtained distribution with the one in the region of missing π°, so imposing a selection on the two protons missing mass (squared) below 0.2 GeV^2/c^4.

Figure 7.14 shows the distribution so obtained, with the results of the same fit, gaussian (in red) for the γ signal and polynomial (in blue) for the background. Even though the gaussian fit does not reproduce the tails, the peak position is correctly found. It is centred around 20 MeV/c^2, closer to zero than in the η case and even narrower.

This means that, in the case of the η decay channel, the momentum resolution of the four particles is worse than for the π° channel, and there are systematic deviations which move the missing γ peak at positive mass values. We will see that this effect is more pronounced in the experimental data, where we know that the momentum resolution was worse than in simulation.

In order to study the η electromagnetic channel, and also to evaluate the background contribution, we can plot the proton-proton missing mass (of course without the selection used before) by applying a 3σ selection over the ppe^+e^- missing mass with the fit values shown in Figure 7.13.

Figure 7.15 shows the obtained missing mass distribution. The η and π° peaks are prominent and the background is kept low. In order to find the meson parameters the distribution was fitted over the whole mass range, by using a combination of two gaussian functions, one for the η (blue) and one for he π° (red) peaks, plus a polynomial background (green).

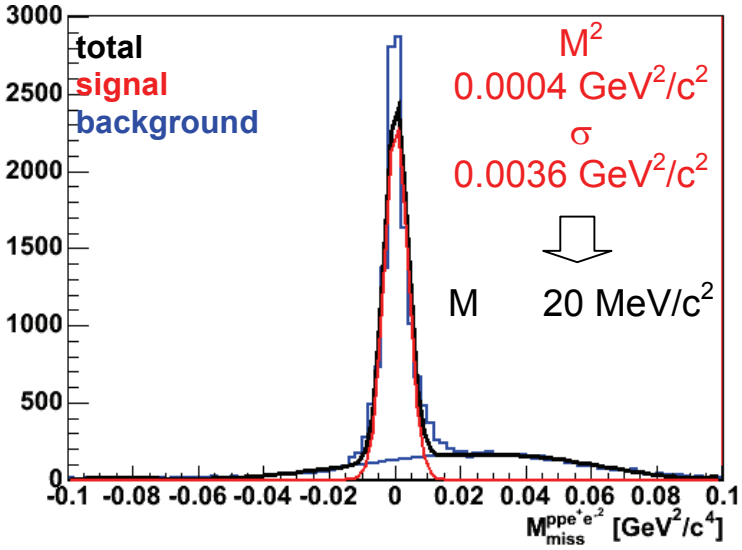

Figure 7.14 – ppe$^+$e$^-$ missing mass squared distribution in the missing π° region, for simulation data ($M_{miss}^{pp\ 2} < 0.2\,GeV^2/c^4$).

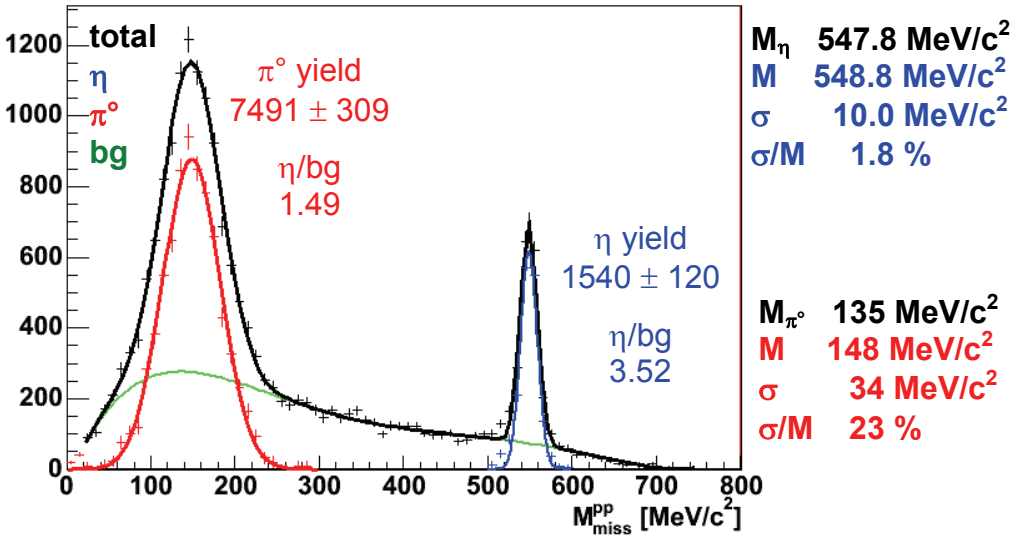

Figure 7.15 – Proton-proton missing mass for simulation data, after a 3σ selection over missing γ mass.

The background is not easy to evaluate in the low mass region, below the π° peak, because at mass values below 50 MeV/c^2 the distribution drops down due to the fact we are evaluating the square root of a number ($M_{miss}^{pp\ 2}$)[6], which can also have negative values (which are rejected in order to perform the computation). Thus we can state that the background evaluation can be misleading in the π° region, and so even the π° yield.

Nevertheless the fit function (black line) fits well the distribution. The η meson is peaked at 548.8 MeV/c^2 with a width of 10.0 MeV/c^2, that is at the correct position; the

[6] As an example if we have a distribution constant in x, the distribution over $\sqrt{x}$ will decrease toward zero values, because of the $x > 0$ condition that we impose to calculate the square root.

mass resolution so obtained is 1.8%. By integrating the fit function less the background we can estimate, in a 3σ mass range around the peak, 1540 ± 120 η events, with a signal over background ratio of η/bg ~ 3.52.

About the missing π° meson, we can see that its position is at 148 MeV/c^2 (width 34 MeV/c^2), distant from the correct position of 135 MeV/c^2. This effect is mainly due to the proton momentum loss while crossing the materials around the target region.

In general the particle momentum is reconstructed from the trajectory deviation inside the magnetic field region; effects of energy loss in air and inside MDC chambers are negligible. But before reaching the MDC chambers and the field region, after the particle is emitted inside the target it must cross all the materials placed around that region, mainly the RICH detector. In this region the particle loses energy and momentum, according to its original momentum and its mass.

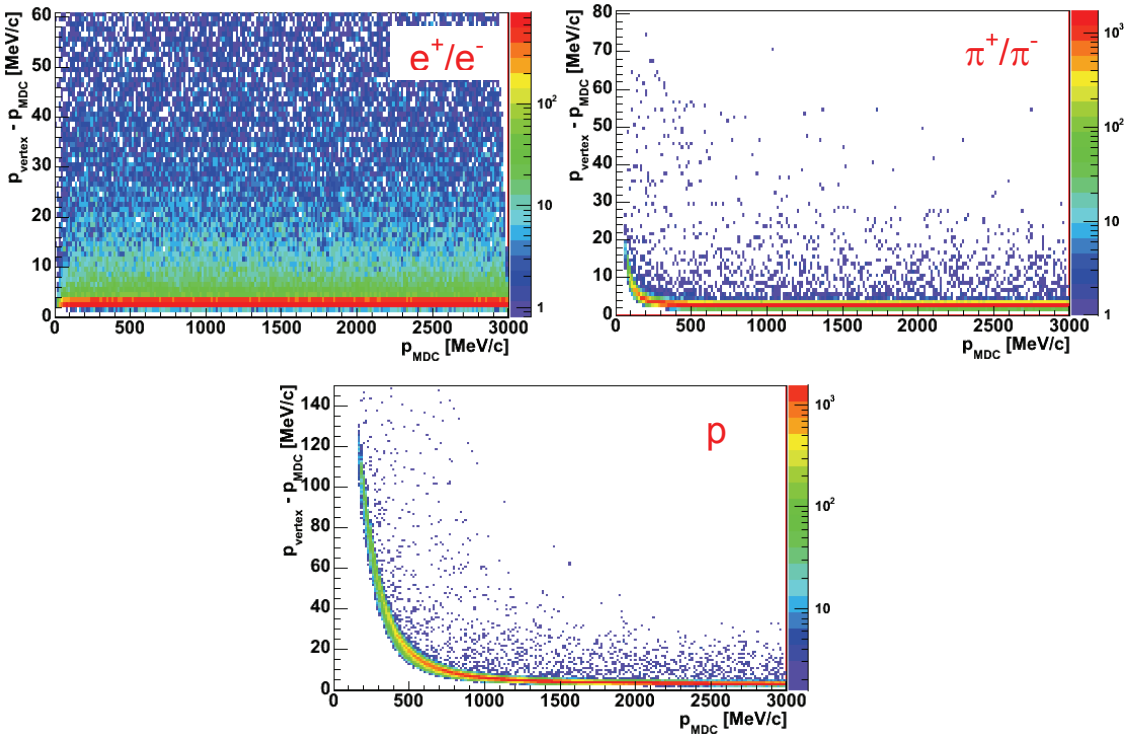

Figure 7.16 - Difference between the proton momentum evaluated at the reaction vertex and in the first layer of MDC1, as a function of the momentum in MDC. Plots were made by using HGEANT simulation, for different kinds of particles.

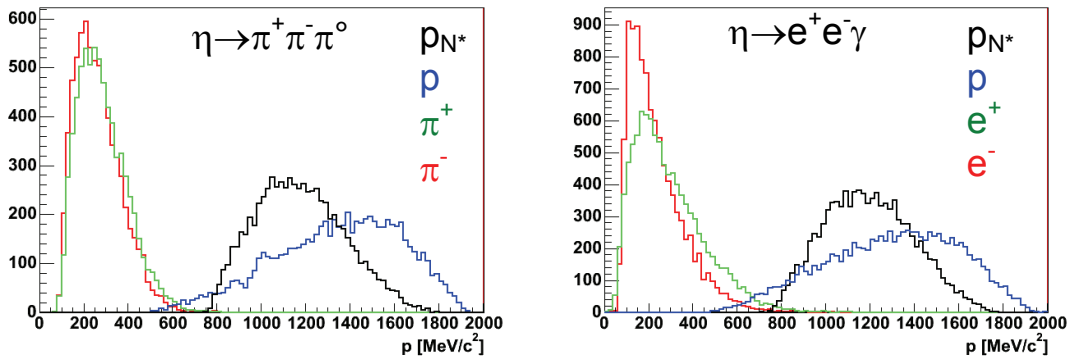

Figure 7.17 – Momentum distribution for final state particles coming from η meson decays, hadronic (on the left) and electromagnetic (on the right) ones, tracked inside HADES acceptance.

By means of the HGEANT simulation it is possible to evaluate the particle momentum at each point of its trajectory. In Figure 7.16 the difference between the particle momentum when emitted at the vertex and when they cross the first layer of MDC1 (i.e. the momentum loss) are plotted as a function of the MDC momentum value (i.e. the reconstructed one), for electrons/positrons, pions and for protons.

While for leptons the momentum loss is negligible, and the same is also for pions up to 100 MeV/c^2, the effect of momentum loss for protons becomes stronger for reconstructed momentum values below 500 MeV/c^2.

The proton momentum loss does not play a role in elastic scattering analysis, because the proton pair acceptance covers the momentum region above 800 MeV/c^2, and it can be ignored in η decay, where protons have at least 500 MeV/c^2 (see Figure 7.17).

In the π° decay this effect becomes important. We can select protons coming from $pp e^+e^-$ events, with pp missing mass below 400 MeV/c^2. In the left plot of Figure 7.18 we can see the difference between the reconstructed and the *real* (from simulation) momentum of protons, plotted as a function of the correct one. The effect at momentum values lower that 500 MeV/c^2 is visible, it makes the reconstructed momentum underestimated and widens the missing π° mass peak.

On the right plot of Figure 7.18 we can see the same plot but this time using momentum values from the kinematic refit. By applying the refit procedure the discrepancy is somehow recovered.

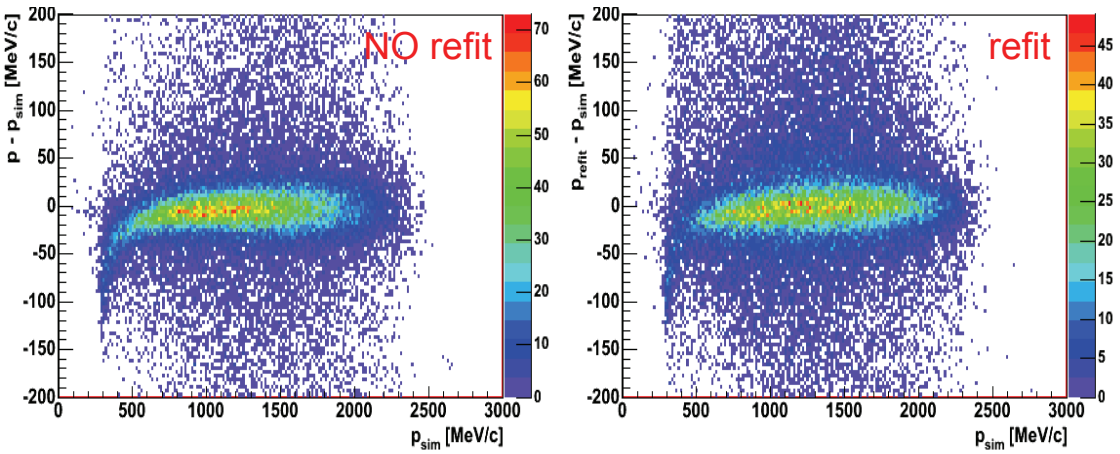

Figure 7.18 – Difference between the reconstructed momentum value and the real one (from simulation) for protons, plotted as a function of the real momentum. On the left plot the distribution is made using Runge Kutta momentum; on the right after the kinematic refit. The deviation at low momenta is partially recovered by the refit procedure.

Figure 7.19 shows the comparison between the pp missing mass distribution without kinematic refit and after applying the procedure. The η peak seems almost unchanged, while the π° peak is now narrower and centred at lower mass values, much closer to the correct position.

In Figure 7.20 we can look at the distribution with only the kinematic refit missing mass values. The distribution was fitted by the combination of two gaussian functions for the meson peaks plus a polynomial background.

The η meson peak is centred at 546.0 MeV/c^2 (548.8 MeV/c^2 before the refit) and with a width of 10.6 MeV/c^2 (against 10.0 MeV/c^2 before). The η yield at 3σ is 1453 ± 116, and the signal/background ratio is 3.08 (previously 3.52). From the comparison

between the obtained values before and after the kinematic refit we can state that the η meson values become a little worse than before, but the difference is minimal.

For the π° peak the centre is closer to the correct place, now at 137 MeV/c^2, while the width from 34 MeV/c^2 (23%) becomes 21 MeV/c^2 (15%). The π° yield is now 8242 ± 290 in a 3σ mass region, and the signal/background ratio is 2.36 (to be compared to the old 1.49 factor).

The kinematic refit improved a lot the distribution, even if only in the π° region. In the experimental data we will see that the effect becomes important also for the η meson.

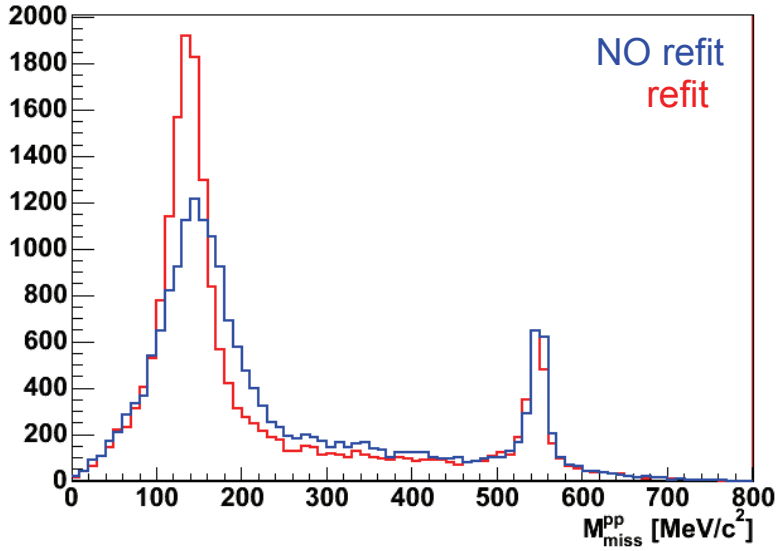

Figure 7.19 – Comparison between pp missing mass distribution before (blue) and after (red) kinematic refit procedure. While the η peak is almost unaffected, the π° peak has improved in terms of centre position and width.

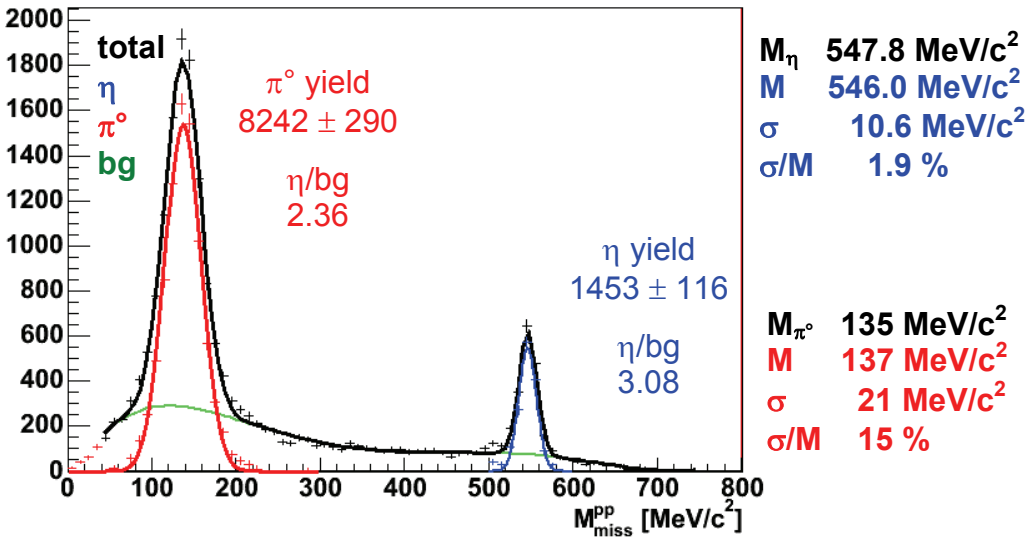

Figure 7.20 – Proton-proton missing mass distribution after kinematic refit.

Once we are able to select the pp→ppη reactions, we must understand which kind of lepton pairs we have in our data sample. By means of our missing mass selections we are able to distinguish events containing pp→ppη, η→$e^+e^-\gamma$ decay channels; while it

could seem obvious to state that we are selecting η Dalitz decays, we must consider that an e^+e^- pair can come even from a conversion process.

Real photons can interact with the materials of the spectrometer (or even with air) and produce conversion pairs $\gamma \rightarrow e^+e^-$. The η meson can decay into two gamma rays $\eta \rightarrow \gamma\gamma$ (branching ratio 39.4%), and one of them (even both) can produce a conversion pair; in this case the ppe^+e^- missing mass will be centred at zero (we miss a photon) and the pp missing mass distribution will give us the η meson value. Thus from a missing mass analysis we cannot separate these two different processes. This is the reason why there are not so many papers on the η form factor by using $\eta \rightarrow e^+e^-$ Dalitz decay.

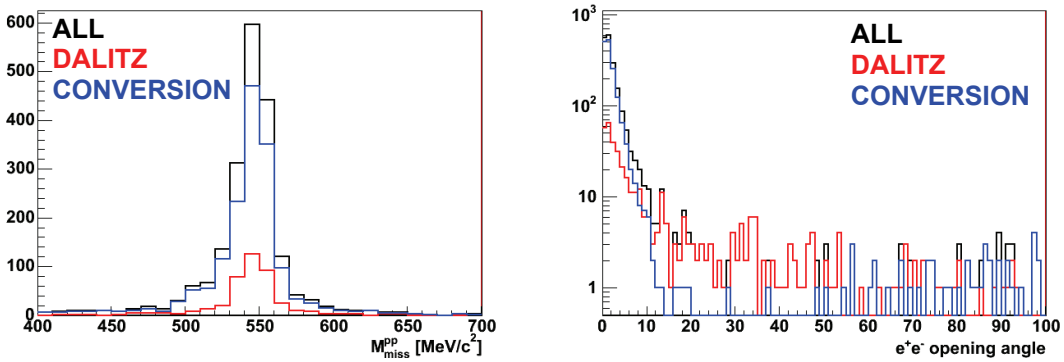

Figure 7.21 – pp missing mass distribution for η decays (on the left), by separating the contribution of the Dalitz decay (in red) from conversion processes (in blue). On the right the e^+e^- opening angle distribution.

In order to understand the contamination we can check by simulation which processes produced the outgoing electrons/positrons. In the left plot of Figure 7.21 the pp missing mass is showed only for η decays, separately for η Dalitz and γ conversion decays. We can see that most of our counts come from conversion processes.

In general the leptons coming from conversion pairs have a small opening angle. The right plot of Figure 7.21 shows the opening angle distribution for dilepton pairs, separately for each sources. We can see that conversion pairs have opening angles lower than 10°; a reduced contribution at higher angles is still present, coming from combinatorial background (leptons coming from different photons).

In general in C+C experiments a selection on opening angle $\alpha > 9°$ is used to reject most of the conversion pairs. Table 7-3 shows the number of η decays coming from different processes, as evaluated by simulation (no 3σ missing mass selections). We can see that without any selections the yield is dominated by conversion pairs, only 20% of the data sample is constituted by Dalitz decays.

The opening angle selection cuts away most of the conversion pairs, only 5% survive after the selection. By applying the 9° opening angle cut, 37% of Dalitz decays survive, but there is still a 34% of conversion processes in the data. This means that in the next future, in order to evaluate correctly the contribution from conversion and to isolate the Dalitz decays, a much deeper analysis is needed on the selection criteria.

Moreover, the conversion processes strongly depend on our knowledge about the detector materials, which are set in HGEANT software. Thus simulation numbers can differ considerably from what really happens in the experiment: in no way we can reliably extrapolate the conversion contribution from the simulation to the experiment.

Table 7-4 shows the summary about the all the values obtained for the exclusive reconstruction of the η electromagnetic decay channels in simulation; values for π° are also shown. We can see that by applying also the 9° opening angle cut the number of

reconstructed η meson goes down to 161 ± 41. The η peak becomes a little broader (12.3 MeV/c^2), mainly because of the lower statistics and therefore larger errors in the fit.

By checking the π° yield we can see a reduction of about 6% as compared to the numbers before the angle cut, while the reduction for η is 11%. We must consider that π° has a lower mass and then the corresponding average opening angle of the outgoing lepton pair is narrower than for η; thus with the opening angle selection we are cutting more π° than η signals.

The same analysis now will be performed with the experimental data.

	No cut	α > 9°	Reduction
ALL	2044	234	11 %
DALITZ	418	155	37 %
CONVERSION	1626	79	5 %
DALITZ / ALL	20 %	66 %	

Table 7-3 – Number of η decays coming from different processes, with and without a selection in opening angle. The reduction is calculated dividing the number of events with α>9° by the number of events without the angular selection.

		Mass [MeV/c^2]	σ [MeV/c^2]	σ/M	yield	η/bg
η	NO refit	548.8	10.0	1.8	1540 ± 120	3.52
	refit	546.0	10.7	2.0	1453 ± 116	3.08
	α>9°	544.5	12.3	2.3	161 ± 41	4.03
π°	NO refit	148.2	34.1	23.0	7491 ± 309	1.49
	refit	136.8	21.5	15.7	8242 ± 290	2.36
	α>9°	132.1	21.8	16.5	557 ± 81	2.68

Table 7-4 - Summary of the results from the exclusive reconstruction of η electromagnetic decay in simulation data. The π° values are also shown.

7.3.2 Experimental data

In Figure 7.22 the two-dimensional missing mass plot is shown. We can see that the background is higher than in simulation, as we should expect, but nevertheless the η meson bump is visible and it can be separated from the other sources.

A proton-proton missing mass range was selected between 0.27 GeV^2/c^4 and 0.33 GeV^2/c^4, like with the simulation data, in order to focus on the η peak region and to evaluate the four particle ppe^+e^- missing mass, as shown in Figure 7.23.

It is evident that the background is much higher than in the simulation, but the missing γ peak is visible. The experimental distribution was fitted by a gaussian function for the photon peak (in blue) plus a polynomial function for the background

(in red). It has to be underlined that the main peak is not centred at zero, as we should expect, but is shifted toward positive values and much more than in the simulation.

We can calculate that the centroid position of the missing γ corresponds to a missing mass value of 91 MeV/c^2, therefore it is shifted toward higher mass values even more than in simulation data. In the next future this effect will have to be investigated with a much deeper analysis of the tracking code.

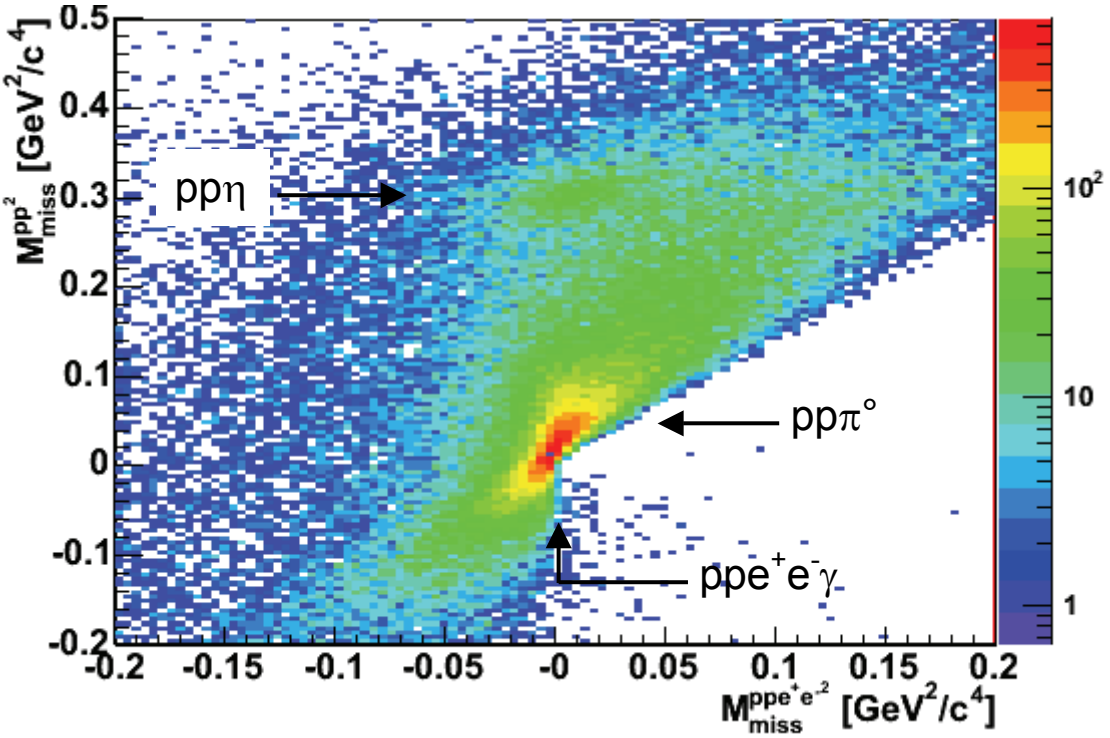

Figure 7.22 – Missing mass plot for four detected particles (ppe$^+$e$^-$) in experimental data. All the visible reaction channels are indicated in the plot.

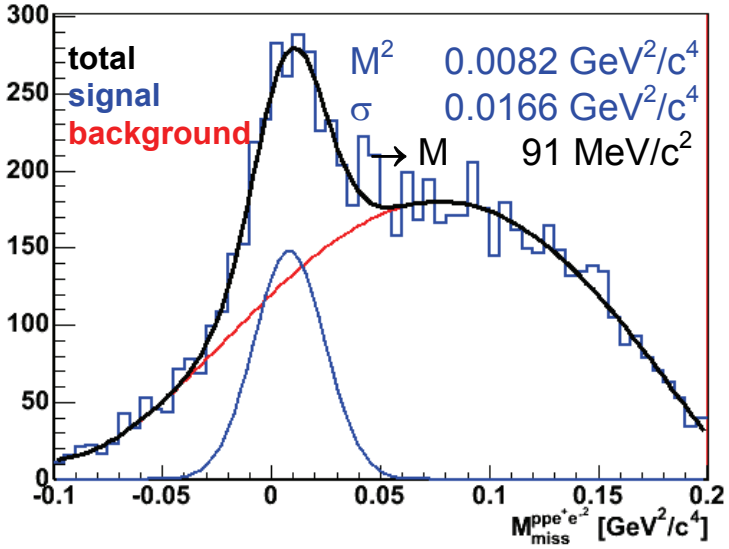

Figure 7.23 – ppe$^+$e$^-$ missing mass (squared) distribution for experimental data, after the selection $0.27\,GeV^2/c^4 < M^{pp}_{miss}{}^2 < 0.33\,GeV^2/c^4$ (η peak).

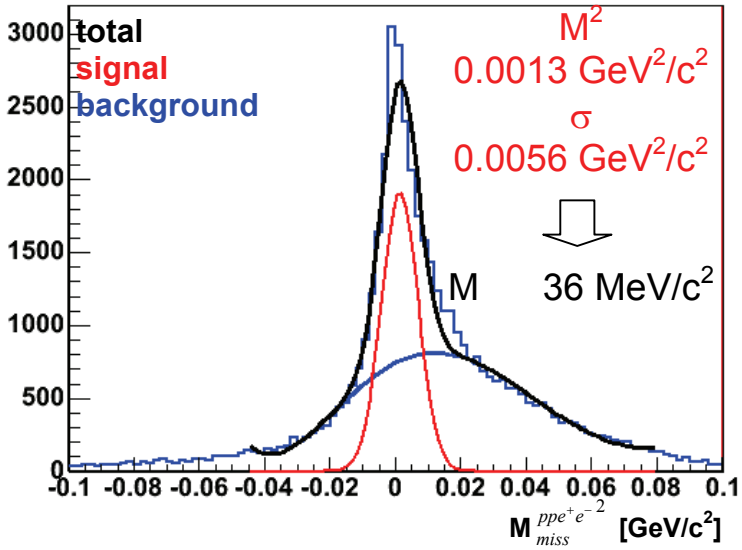

Figure 7.24 – ppe$^+$e$^-$ missing mass squared distribution in the missing π° region, for experimental data ($M_{miss}^{pp\ 2} < 0.2 GeV^2/c^4$).

If we look at the ppe$^+$e$^-$ missing mass distribution in the region of the missing π° ($M_{miss}^{pp\ 2} < 0.2 GeV^2/c^4$), we can see that the displacement (36 MeV/c^2) is reduced with respect to the η meson region.

By applying the same procedure as used in simulation, we can make a 3σ selection over the four particle missing mass around the missing γ, using the fit parameters from the distribution in Figure 7.23.

The missing π° peak is totally dissolved by a low resolution momentum reconstruction, probably due to the proton momentum loss, nevertheless the η meson peak is still well defined.

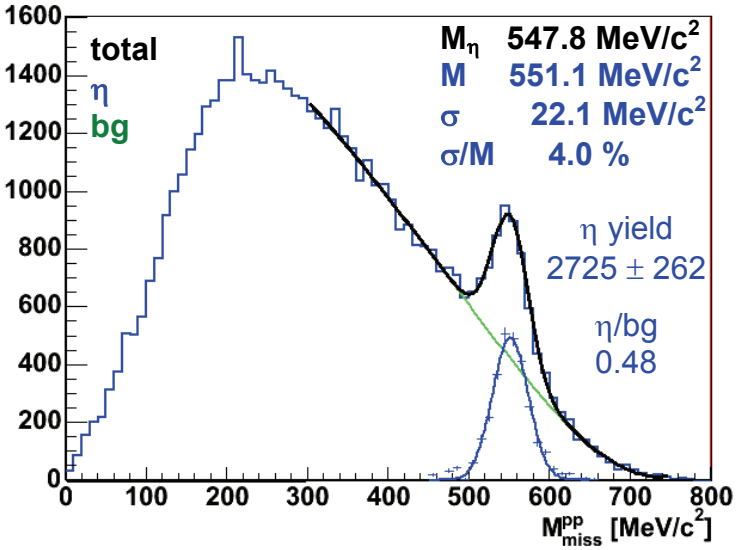

Figure 7.25 – Proton-proton missing mass distribution for experimental data, by applying a 3σ cut on the ppe$^+$e$^-$ missing mass around the γ peak. The π° peak is completely melted by a low resolution momentum reconstruction.

The experimental distribution was fitted by a polynomial background (green line) plus a gaussian function (in blue) for the peak.

The peak is centred at 551.1 MeV/c^2 with a width of 22.1 MeV/c^2. The achieved mass resolution of 4% is comparable with the one obtained via the hadronic decay (3.6%). The η yield inside a 3σ pp missing mass range is 2725 ± 262, with a signal/background ratio of 0.48.

The distribution is improved by the kinematical refit procedure, as shown in Figure 7.26. The refit is able to move the proton momenta toward the correct values, the peak of the missing π° is now clearly visible and the η peak is now better resolved.

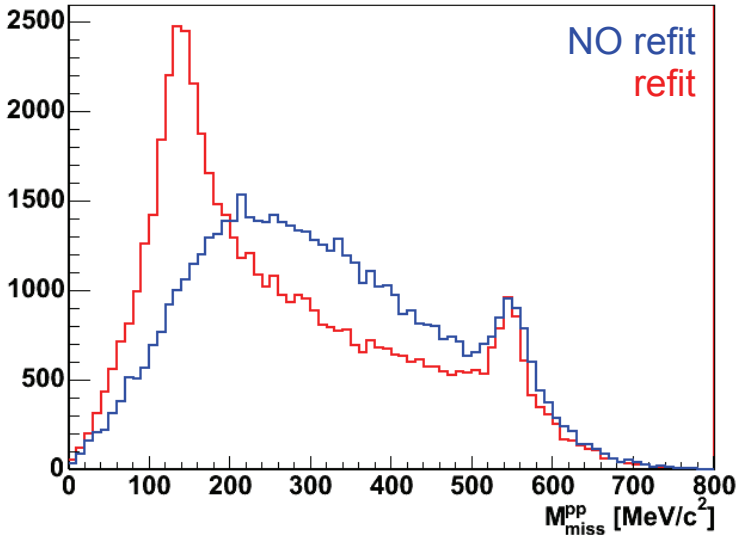

Figure 7.26 – Comparison between pp missing mass distribution with (red) and without (blue) kinematic refit. After the refit procedure the missing π° is clearly visible.

Figure 7.27 shows the kinematical refit distribution, now fitted also in the π° region. The η meson peak is now centred at 546.0 MeV/c^2, and the width is reduced to 17.8 MeV/c^2 (against the previous 22 MeV/c^2 value). The mass resolution corresponds to 3.3 % (previously it was 4.0%), which is a bit higher than the 2.5% for the hadronic decay, but still consistent with the elastic scattering analysis. The reason of this discrepancy mainly depends on the different proton kinematics, and it will need a more accurate study for a refined analysis.

Nevertheless the achieved missing mass resolution is in agreement with the value obtained via the elastic scattering analysis for the proton-proton invariant mass (see table 5-5), where for experimental data we evaluated 2.8 % for the sector pair 1-4, 2.3% for sectors 2-5, and 5.9% for the 3MDC sector pair 3-6. When reconstructing the η channel we combine the momentum measurement of four charged particles which hit different sectors; therefore our final mass resolution is averaged over the resolution of all the involved sectors. It is evident that the low resolution of sector 3 worsens the overall average mass resolution value.

The same fit procedure can be repeated for all the trigger combinations which were used during the data acquisition, such as downscaled first level triggered events (**Ds**), second level triggered events (**LVL2**), downscaled events with a positive 2nd level trigger decision (**LVL2Ds**), and by applying a condition on the e^+e^- opening angle α >9°.

Table 7-5 shows a summary of all the values obtained by fitting experimental distributions, for both η and π° mesons.

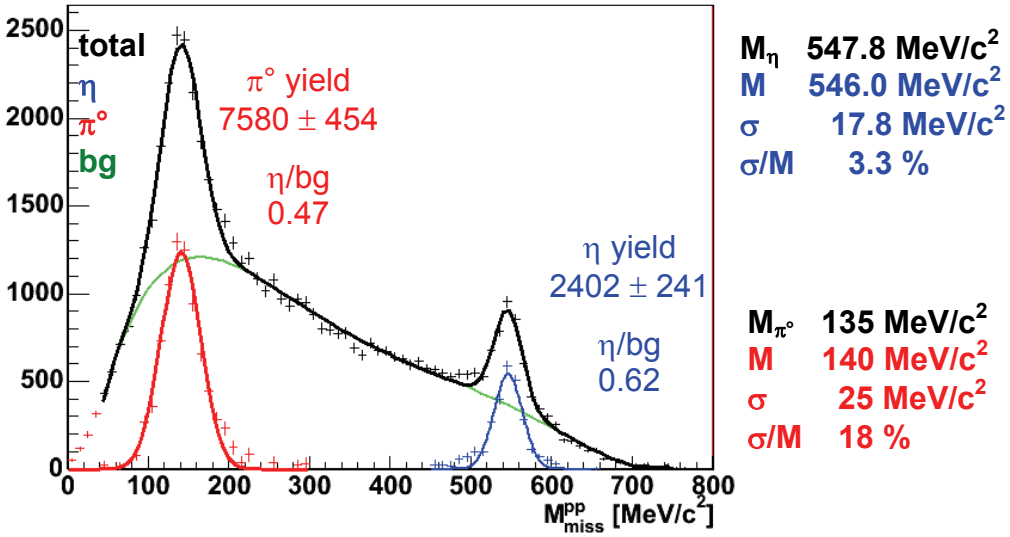

Figure 7.27 – Proton-proton missing mass distribution after kinematic refit, for experimental data.

		Mass [MeV/c²]	σ [MeV/c²]	σ/M	yield	η/bg
η	NO refit	551.1	22.1	4.0	2752 ± 262	0.48
	Refit	546.0	17.8	3.3	2402 ± 241	0.62
	Ds	545.5	18.0	3.3	1220 ± 176	0.60
	LVL2	546.4	17.4	3.2	2175 ± 224	0.62
	LVL2Ds	545.8	19.0	3.5	1053 ± 163	0.58
	α>9°	543.3	23.7	4.4	303 ± 72	0.80
	α>9° Ds	546.5	24.2	4.4	164 ± 51	0.90
	α>9° LVL2	544.0	23.8	4.4	295 ± 70	0.81
	α>9° LVL2Ds	548.2	25.2	4.6	160 ± 23	0.91
π°	NO refit	-	-	-	-	-
	Refit	140.2	24.6	17.6	7580 ± 454	0.47
	Ds	140.5	24.3	17.3	3997 ± 343	0.48
	LVL2	140.3	24.6	17.5	6898 ± 433	0.47
	LVL2Ds	141.0	26.0	18.4	3530 ± 320	0.49
	α>9°	132.6	22.9	17.3	644 ± 104	0.79
	α>9° Ds	136.6	26.9	20.4	381 ± 78	0.94
	α>9° LVL2	131.9	22.3	16.9	583 ± 97	0.76
	α>9° LVL2Ds	135.5	27.7	20.4	323 ± 73	0.82

Table 7-5 – Summary of the results from exclusive reconstruction of η electromagnetic decay in experimental data.

We can see that peak centroids and width values are stable according to different trigger selections. By applying the opening angle cut the statistics of the η meson drops down, therefore the worse resolution values and error bars are connected to a higher

uncertainty coming from the peak fit. But we have to notice that the values do not change so much, showing that the full analysis is consistent.

An open question about the spectrometer setup is the efficiency of the 2nd level trigger, in order to understand how many dilepton events we lose by using the lepton trigger for the data acquisition.

For this kind of analysis we need to use events which are triggered by the downscaling box (see chapter 4), so that they do not depend on the LVL2 decision.

By selecting only downscaled events, we can evaluate how many η mesons are reconstructed in the whole sample (Ds), and in downscaled events which had a positive 2nd level trigger decision (LVL2Ds). By dividing these numbers we obtain an estimate of the efficiency ε_η for η reconstruction:

$$\varepsilon_\eta = \frac{LVL2Ds_\eta}{Ds_\eta} \qquad \textbf{(Eq. 7-4)}$$

The same method can also be applied to evaluate the efficiency ε_{π° for the neutral pion, even if the estimate is less accurate because of the difficulty of background evaluation.

In this way we obtain $\varepsilon_\eta = 0.86 \pm 0.18$, $\varepsilon_{\pi^\circ} = 0.88 \pm 0.11$. The large error bars are related to the error propagation of the parameters coming from the fit. Nevertheless the two obtained values are close to each other and this means that the trigger efficiency estimate is consistent[7].

Hadronic and electromagnetic η decay yields can be evaluated, even if we cannot compare the values to the expectation from the branching ratio values, because at the moment we are not able to isolate the Dalitz decay from the contamination of conversion pairs.

The ratio between hadronic and electromagnetic decay channels can be calculated in simulation by simply dividing the numbers obtained from the η fits, which can be found in Table 7-2 and Table 7-4. In this way we obtain a factor 15.3 ± 1.3 as hadronic/electromagnetic ratio.

In the experiment the same ratio can be calculated with two different methods, by using values from Table 7-2 and Table 7-5.

If we select only downscaled events, we can compare the yields by using the same data sample[8]. By simply dividing downscaled yields we obtain a hadronic to electromagnetic ratio of 18.7 ± 2.9.

Another way consists of using the electromagnetic decays in the 2nd level triggered events. In this case the electromagnetic yield has to be corrected by the trigger efficiency (86 % as previously calculated), while the hadronic channel has to be rescaled to the total number of LVL1 triggered events, therefore it has to be multiplied by the average downscaling factor (2.2). The correct formula is:

$$\frac{\eta_{hadronic}}{\eta_{electromagnetic}} = \frac{\eta_{hadronic}^{Ds} \cdot downscaling}{\eta_{electromagnetic}^{LVL2} \Big/ \varepsilon_\eta^{LVL2}} \qquad \textbf{(Eq. 7-5)}$$

[7] In general the trigger efficiency depends also on the pair opening angle; with the present fit values, for reconstructed mesons with opening angle larger than 9° the errors are too large to evaluate a reliable efficiency (mainly due to the low number of counts, in particular for η).

[8] Hadronic decays were reconstructed by using only downscaled events.

With this method we obtain a hadronic/electromagnetic factor of 19.8 ± 2.1, which agrees with the value found using downscaling events within the error bars.

At the moment we can state that our experimental ratio is higher than the simulation one. If we consider the electromagnetic channel the one which differs between experiment and simulation, the discrepancy means that in the experiment we are reconstructing only about 80% lepton pairs with respect to the simulation. This is reasonable considering that the RICH efficiency is not yet well understood, and we suspect it has a lower efficiency value than in simulation. Therefore at the moment our electromagnetic sample is contaminated by spurious conversion events, which does not allow us to provide quantitative considerations about normalization factors.

Nevertheless, the two ratios obtained in the experimental data with the two methods agrees, and this means that the evaluated 2^{nd} level trigger efficiency is reasonable; moreover the simulation and experimental ratios are not quite different, thus it is possible to state that the analysis is in a good shape and soon our final normalization factors could be extracted.

7.4 Exclusive η reconstruction summary

In this chapter the whole procedure for the η exclusive reconstruction was presented, for both hadronic and electromagnetic decay channels.

The procedure is based first on the selection of events with the interesting four particles in the exit channel ($pp\pi^+\pi^-$ for the hadronic decay, ppe^+e^- for the electromagnetic decay); in a second stage the four particle missing mass is plotted in order to find the missing particle of the reaction, a neutral pion for $\eta\rightarrow\pi^+\pi^-\pi^\circ$, a photon for $\eta\rightarrow e^+e^-\gamma$; after the missing particle is found, the missing mass for the two outgoing protons is plotted in order to select $pp\rightarrow pp\eta$ reactions. By means of a fit procedure the individual contributions to the interesting events and to the background are evaluated, and then the invariant mass resolution and the meson yields can be calculated. A kinematic refit procedure is applied in order to improve the mass resolution, by imposing a kinematic constraint on the reaction of interest.

The hadronic decay channel analysis showed a well defined η peak (signal/background 0.57), centred at the correct position with an invariant mass resolution of 2.5 %. This value is perfectly in agreement with what obtained by the elastic scattering analysis of chapter 5, and it demonstrates the good status of the HADES tracking system and momentum reconstruction. With the fully analysed data sample we are able to reconstruct about 22,000 η hadronic decay events.

By means of the electromagnetic analysis we demonstrated that with the spectrometer we can select exclusively the η decay channel with good performances, achieving an invariant mass resolution of 3.3 % and a signal to background ratio of 0.62. Some problems occur in the π° meson reconstruction without kinematic refit, where the peak spreads away due to the poor resolution; the reason of this effect is well understood and it is connected to the momentum loss of low momenta protons while crossing target and RICH, which is not visible in elastic and η meson reactions. In the near future a momentum dependent correction is foreseen, however at the moment the kinematic refit procedure is able to correct the problem providing a satisfactory π° peak.

Coming back to the electromagnetic channel, we estimated about 2,400 η electromagnetic decays in our experimental data sample. From our simulations we

know that most of these events come from gamma conversion processes, and a limited part is due to true η Dalitz decays. From the simulation we evaluated that the Dalitz channel could be scaled by about a factor 5 in the total yield; by selecting only lepton pairs with opening angle greater than 9° we see that the contribution from conversion processes is reduced but still present, therefore at the moment it is not possible to make any consideration about the η Dalitz decay alone.

The obtained invariant mass resolution values for the hadronic and electromagnetic channels are in agreement with each other, and also with the elastic scattering analysis. The exclusive reconstruction procedures are working and they provide good performances, in order to select the desired channels. Now all the instruments are ready in order to perform physical analysis on the January 2004 data, and in particular on η meson decays.